

# FAULT-RELATED INSTABILITY PROBLEMS OF TUNNELS - THE HOST ROCK SLIP CRITERION AND CHARACTERISTICS OF THE TUNNELING-INDUCED SHEAR DISPLACEMENTS

*Jian-guo Liu, Xiao-jun Zhou, Qing-hua Xiao and Wei Zhao*

*Key Laboratory of Transportation Tunnel Engineering of Ministry of Education, School of Civil Engineering, Southwest Jiaotong University, Chengdu, 610031, China, email: xqh\_bp@163.com*

## ABSTRACT

As one of the fault-related instability problems of tunnels, rock slip along fault plane is closely related to the shear strength of a fault, and usually causes irrecoverable and sometimes catastrophic engineering problems. In this paper, based on continuum assumption and Coulomb-slip failure, a criterion to evaluate rock slip along the fault plane was proposed for a circular tunnel in rock masses containing a fault. A mathematical equation that describes the relationship between required shear strength of a fault and horizontal stress ratio, fault spatial extension and location was established. From the equation, the influences of the important parameters on the required shear strength of a fault was analysed after a numerical validation was performed. Besides, the effects of fault spatial extension and location on the tunnelling-induced shear displacements were characterized through numerical models. Characteristics of the tunnelling-induced shear displacements at the excavation wall indicated that fault location with respect to the tunnel dominates the nonuniform rock deformations at excavation wall, and larger fault dip angles could lead to larger shear displacements in some specific pair cases. The presented investigation provides both a deeper insight into the instability problems of tunnels related to a fault and a guideline for tunnel support design.

## KEYWORDS

Tunnel, Fault-related instability problem, Rock slip criterion, Fault shear strength, Tunnelling-induced shear displacement

## INTRODUCTION

Fault is quite common in all types of hard rock masses, which affects the mechanical properties of rock mass greatly. Many failures or instability problems of tunnels reported are related to the nearby fault presence [1-4]. And the instability of host rock around tunnel usually led to irrecoverable and catastrophic results. Fault-related instability of underground openings are often presented as rock slide along the fault plane, the downfall of blocks, wedges cut by faults or minor joints inward the cavern[5-7]. Among these types of instability, rock slide along the fault plane is a severe problem that can cause irrecoverable failure and may be a severe threat on long-term stability

of underground openings [1,4,8,9]. A better understanding of this problem is therefore highly required and urgent in the determination of support design for tunnels. Typical structural failure of a tunnel caused by the rock slip is presented in Figure 1.

Attempts have been made to assess the fault-related problems by empirical or semi-quantitative methods such as rock mass classification [10] and limit equilibrium approach with the aids of stereographic projection and blocky theory [11, 12]. Numerical models and physical model tests were used more often as specific academic or engineering problems could be assessed much easier than many parameters could be taken into consideration. When tunnelling in hard rock containing faults, uneven rock pressures usually cause asymmetrical stress distribution in tunnel support [13 - 16], which is not favourable and even resulted in failure as the support is designed to be symmetrical. And rock failure or the uneven rock pressures acting on support are usually due to nonuniform rock deformations [17, 18], or shear behaviours of rock along the fault plane more precisely [7, 19].



*Fig. 1 - Liner failure caused by rock slide along fault [7]*

Shear behaviour of rock, also characterized as rock slip along the fault plane, is a typical response to insufficient shear strength of a fault. And in the researches of Yeung et al. [20], Hao et al. [21] and Wang et al. [22], the shear strengths of faults or joints were pointed out to have a dominant influence on the stability of rock. Furthermore, the appearance of rock slip did not seem to be just only dependent on the fault shear strength. More detailed analysis that considered some other important parameters of horizontal stress ratio, fault dip and fault location were performed too [22 - 24]. The consideration of other parameters revealed that, for a given fault shear strength, the stability of rock could not be determined when other parameters were not specified, and the required fault shear strength to keep rock stability showed dependency on stress ratios, fault dips and fault locations.

Given this background, the fault-related instability problems of tunnels need further investigation. Firstly, the spatial extension and location of a fault with respect to the tunnel needs to be characterized more precisely to enable the theoretical analysis of the problems. Secondly, the required fault shear strength is highly dependent on the stress ratio, fault dips and locations, and then the relationships among these parameters need to be addressed clearly. Besides, the

tunnelling-induced shear displacements at excavation wall resulting from relative insufficient fault shear strength were unfavourable to tunnel support. So the effects of the important parameters of horizontal stress ratio, spatial extension and location of a fault and shear strength of a fault on the tunnelling-induced shear displacements should be investigated.

In the present research, the fault spatial extension and location with respect to a tunnel were mathematically characterized firstly, which enabled the stress analysis of rock along the fault plane. And then based on continuum assumption [25], the elastic mechanics solution of rock along the fault plane was carried out. A criterion for circularly tunnelling in hard rock containing a fault that followed Coulomb-slip failure was proposed, which mathematically described the relationship between the required fault shear strength and fault spatial extension, fault spatial location and ground horizontal stress ratio. The required fault shear strength to prevent rock slip (named lower frictional angle of fault  $\theta_{lim}$  when no cohesion was considered), was proposed and validated with numerical models. The effects of fault spatial extension and location and horizontal stress ratio on the lower frictional angle of fault  $\theta_{lim}$  were analysed, which revealed the influences of a fault on the stability problems of tunnels. In addition, the effects of fault spatial extension and location on the tunnelling-induced shear displacements at excavation wall were characterized through numerical models. The attempts of this paper provided a deeper insight into the instability problems of underground openings related to fault slip.

## THE CRITERION OF ROCK SLIP ALONG A FAULT

### Stress analysis on the fault plane

A circular tunnel is selected in this research to simplify the stress analysis. The spatial geometric relationship between the fault and tunnel is illustrated in Figure 2. As the axial size of tunnel is much greater than the radial one, this problem can be simplified as a plain strain problem in the  $yoz$  plane. For a deeply buried tunnel, the tunnel radius  $r_0$  is much smaller than the depth  $h$ , thus the model can be simplified as a problem of stress concentration around a small hole in infinite domain, as presented in Figure 3.

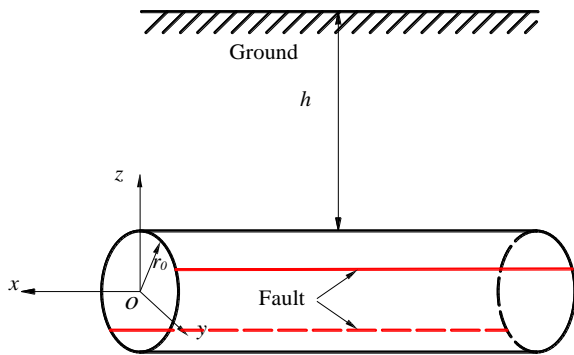


Fig. 2 - Spatial relationship between tunnel and fault

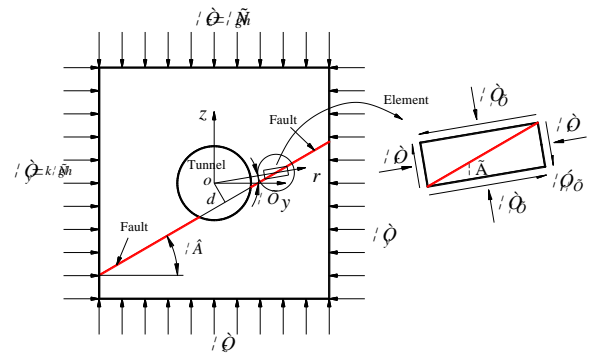


Fig. 3 - Simplified model for plane strain problem

As shown in Figure 3, a circular tunnel is excavated in infinite elastic medium which contains a fault, and the spatial extension and location of the fault could be characterized by dip angle of fault  $\beta$  and the distance between the fault plane and circular tunnel center  $d$ . And special assumptions are made as follows:

- (1) In the initial geostress field, the rock did not slide and the fault did not change the distribution of the initial stress;
- (2) The secondary stress distribution due to the excavation of tunnel is the same as that in rock mass without a fault prior to rock slip.
- (3) No tectonic stress field is considered.

According to the spatial relationship between fault plane and tunnel, for a fault going through the right bottom below the tunnel center, the relationship of fault dip angle  $\beta$  and  $\gamma$  in a polar coordinate system could be expressed as follows:

$$\sin \gamma = d / r = \sin(\beta - \varphi) \tag{1}$$

where  $\gamma$  is the angle between polar radius and fault plane,  $\varphi$  is the polar angle in the coordinate system. When only self-weight of rock mass is considered, the initial geostress can be expressed as:

$$\begin{aligned} \sigma_z &= \rho gh \\ \sigma_x = \sigma_y &= \mu / (1 - \mu) \rho gh = k \rho gh \end{aligned} \tag{2}$$

where  $\rho$  and  $\mu$  are the density and Poisson's ratio of rock mass, respectively. And  $k$  is the horizontal stress ratio.

When a circular tunnel with a radius of  $r_0$  is excavated, the secondary stress distribution in the rock mass containing a fault with a dip angle of  $\beta$  through the right bottom of a circular tunnel (), originally due to Kirsch [26], are:

$$\begin{aligned}
 \sigma_r &= \sigma_z / 2 \times [(1 - \alpha^2)(1 + k) - (1 - 4\alpha^2 + 3\alpha^4)(1 - k) \cos(2\beta - 2\gamma)] \\
 \sigma_\varphi &= \sigma_z / 2 \times [(1 + \alpha^2)(1 + k) + (1 + 3\alpha^4)(1 - k) \cos(2\beta - 2\gamma)] \\
 \tau_{r\varphi} &= \sigma_z / 2 \times [(1 - k) \times (1 + 2\alpha^2 - 3\alpha^4) \times \sin(2\beta - 2\gamma)]
 \end{aligned} \tag{3}$$

where  $\alpha = r_0 / r$ , and  $r$  is the coordinates in a polar coordinate system. For tunnels with D shape or horse-shoe shape, the stress can be analysed with complex valuable system.

An element contains the fault is derived to conduct stress analysis as shown in Figure 3, and the normal and shear stress components on the fault plane calculated based on the assumption (2), are given by:

$$\begin{aligned}
 \sigma_n &= (\sigma_\varphi + \sigma_r) / 2 + (\sigma_\varphi - \sigma_r) / 2 \times \cos 2\gamma - \tau_{r\varphi} \times \sin 2\gamma \\
 \tau &= (\sigma_\varphi - \sigma_r) / 2 \times \sin 2\gamma + \tau_{r\varphi} \times \cos 2\gamma
 \end{aligned} \tag{4}$$

### Analysis of lower limit frictional angle of a fault

Prior to rock slip along the fault plane, according to Coulomb-slip criterion, the stress state must satisfy the following equation:

$$\tau \leq \sigma_n \tan \theta + c \tag{5}$$

where  $\theta$  and  $c$  are the frictional angle and cohesion of the fault, respectively. And by substituting Equation 4 into Equation 5, the following equation is led to:

$$\begin{aligned}
 \tan \theta \geq \{ &[-\alpha^2(1 + k) - (1 - 2\alpha^2 + 3\alpha^4)(1 - k) \times \cos(2\beta - 2\gamma)] \times \sin 2\gamma + (1 + k)(1 + 2\alpha^2 - 3\alpha^4) \times \\
 &\sin(2\beta - 2\gamma) \times \cos 2\gamma\} / \{ (1 + k) - 2\alpha^2 \times (1 - k) \times \cos(2\beta - 2\gamma) + [-\alpha^2(1 + k) - (1 - 2\alpha^2 + 3\alpha^4) \times \\
 &(1 - k) \times \cos(2\beta - 2\gamma)] \times \cos 2\gamma - (1 + k)(1 + 2\alpha^2 - 3\alpha^4) \times \sin(2\beta - 2\gamma) \times \sin 2\gamma \}
 \end{aligned} \tag{6}$$

Where  $\sin 2\gamma = 2\alpha d / r_0 \times \sqrt{1 - (\alpha d / r_0)^2}$  and  $\cos 2\gamma = 1 - 2(\alpha d / r_0)^2$ . Equation 6 denotes the criterion to evaluate whether rock would slide along the fault or not, and it is a local criterion, and not for the rock along the whole fault. For deep hard rock engineering, the fault cohesion was always assigned to be zero [21,27]. And for a simplified analysis, cohesion of fault is not considered ( $c=0$ ) in Equation 6.

By setting the left part in Equation 6 equal to the right one, the local lower limit frictional angle of the fault  $\theta_{lim}$ , which is the local minimum of fault shear strength that prevents host rock of tunnel from sliding along the fault plane, is obtained with no cohesion considered. And for the prevention of rock slip along the whole fault plane, the shear strength of fault should be no less than maximum value of  $\theta_{lim}$ , and then the max lower frictional angle of fault  $\theta_{max}$  is determined as  $\theta_{max} = \max \{ \theta_{lim} \}$ .

According to Equation 6,  $\theta_{lim}$  is dependent on the horizontal stress ratio  $k$ , dip angle of fault  $\beta$  and the distance between the fault plane and circular tunnel center  $d$ . It should be noted that rock slip criterion along fault is proposed for the right half of a fault extending at the right bottom of circular tunnel, and for the left part, similar analysis can be performed by transforming the coordinates in the same way.

### Numerical validation

To validate the proposed slip criterion of host rock and lower frictional angle  $\theta_{max}$ , a numerical model is established where vertical stress  $\sigma_z = 4\text{MPa}$ , horizontal stress ratio  $k=0.5$ , tunnel radius  $r_0 = 5\text{m}$ , fault dip angle  $\beta=30^\circ$ , and distance between the fault plane and circular tunnel center  $d=1\text{m}$ . By substituting the parameters of the example into Equation 6, the local lower limit frictional angle of fault along the fault plane is calculated and shown in Figure 4.

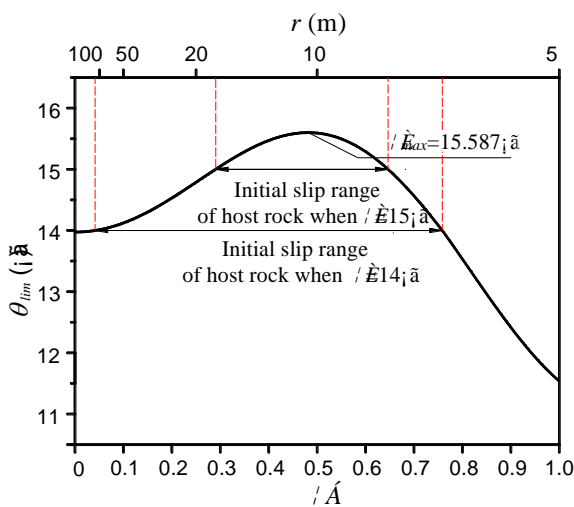


Fig. 4 - Variation of lower limit frictional angle of fault along fault plane

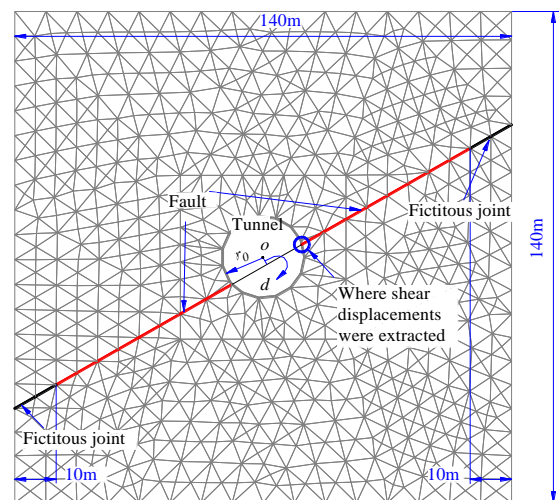


Fig. 5 - Generation of numerical model

Figure 4 illustrated the lower limit frictional angle of fault along the fault plane, which increases firstly and then decreases from excavation wall to infinite in this case. And it can be seen that,  $\theta_{max}$  is located at where  $\alpha \approx 0.48$  in this case, which means that, to maintain the stress distribution at where  $\alpha \approx 0.48$ , the frictional angle of the fault  $\theta$  should be no less than  $15.587^\circ$ . Besides, the initial slip ranges of host rock with different frictional angle of fault were presented in Figure 4. For example, when frictional angle of fault  $\theta=14.0^\circ$  and  $\theta=15.0^\circ$ , the initial slip ranges of host rock are 6.59m~118.17m and 7.74m~17.23m from tunnel center, respectively.

### **Numerical modelling strategies**

The numerical model to validate the criterion proposed is based on the Universal Distinct Element Code (UDEC) [28]. UDEC is a program developed to solve fault-related problems in discontinuous rock system. Large deformation of rock along the fault is allowed and the properties of fault are quite convenient to be changed in this program. With many kinds of built-in constitutive models of fault, UDEC is suitable for the verification of the criterion proposed in Equation 6. In the modelling process, the Coulomb slip model was adopted. In UDEC, if

$$|\tau_s| \leq \sigma_n \tan \theta + c = \tau_{max} \quad (7)$$

Where  $\tau_s$  is the shear stress on the fault plane;  $\theta$  is the frictional angle;  $\sigma_n$  is the normal stress; and  $c$  is the cohesion of fault. Then, the shear displacement can be described as:

$$\Delta u_s^e = \Delta \tau_s / k_s \quad (8)$$

where  $\Delta u_s^e$  is the elastic component of incremental shear displacement; and  $k_s$  is the constant shear stiffness. Or, if

$$|\tau_s| \geq \tau_{max} \quad (9)$$

then

$$\tau_s = \text{sign}(\Delta u_s) \tau_{max} \quad (10)$$

where  $\Delta u_s$  is the total incremental shear displacement.

From Equation 7 to 10, it can be concluded that prior to rock slip along the fault plane, the total shear displacement of rock along the fault is the elastic constant component. And once rock has already slid, the shear displacement is enlarged. Thus, the criterion presented in Equation 6 can be verified by the derivations and comparisons of shear displacements of nodes along the fault in the numerical model.

In the numerical model, rock was assumed to be elastic medium and fault followed Coulomb-slip criterion. Properties of rock mass were taken from the research of Jiang et al. [27], and properties of fault were evaluated under the constant normal stress conditions [29, 30]. In order to prevent the fault from opening, tensile strength of the fault was set at a relatively high value up to 10GPa. Properties of rock mass and fault are presented in Table 1 and Table 2.

Tab. 1 - Properties of rock masses

Density $\rho$ (kg/m <sup>3</sup> )	Young's modulus $E$ (GPa)	Poisson's ratio $\mu$
2.5	3.03	0.17

Tab. 2 - Properties of the fault

Normal stiffness $k_n$ (GPa/m)	Shear stiffness $k_s$ (GPa/m)	Cohesion $c$ (MPa)	Frictional angle $\theta$ (°)	Tensile strength $\sigma_{ten}$ (GPa)
20	0.8	0	Varies	10

Stress boundaries were applied to the model, and horizontal stress ratio  $k$  was simulated by inputting different horizontal stress while vertical stress remained constant. A circular tunnel of  $r_0 = 5m$  was excavated in the rock mass, and in order to eliminate the boundary effect, size of model was set at 140m×140m. Besides, fictitious joint segments were generated near the boundary of model to stabilize the boundary [31], with 10m-long projection on the horizontal axis. The numerical model was generated as shown in Figure 5. The frictional angle of fault  $\theta$  put into the numerical model was in a narrow range near the maximum lower limit frictional angle  $\theta_{max}$ .

### Shear displacements along the fault plane

The shear displacements of nodes along the fault plane  $D_s$  in the 7 cases are presented in Figure 6. For cases with  $\theta / \theta_{max} \geq 1.00$ , the displacement curves are almost the same, which means that the shear displacements of the same node are constant and from elastic shear behaviour according to Equation 7 and 8. While for cases with  $\theta / \theta_{max} < 1.00$ , the shear displacement curves increases gradually within the middle range, which means that the host rock has slid already and stepped into the plastic shear stage according to Equations 9 and 10. It could be summarized that, when the frictional angle of the fault is larger than  $\theta_{max}$ , the stress distribution of host rock could be maintained and rock slip along fault plane is prevented, otherwise the rock slip occurs.

Also in Figure 6, when  $\theta / \theta_{max} = 0.96 \rightarrow \theta = 14.96^\circ$ , the simulated rock slip range is  $r \approx 7m \sim 33m$ , which shows a great disparity compared to that in Figure 4. This difference could be attributed to the stress redistribution effect: when  $|\tau_s| \geq \tau_{max}$  for a fault element, part of  $\tau_s$  would be transferred to neighbouring elements, causing the shear failure of the neighbouring elements, and then the slip range of host rock is enlarged.

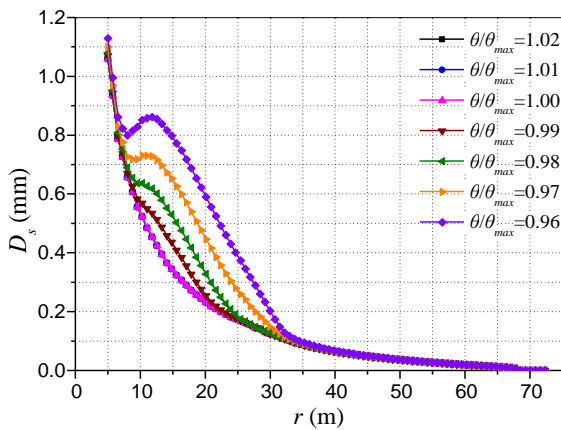


Fig. 6 - Shear displacements of rock along fault plane

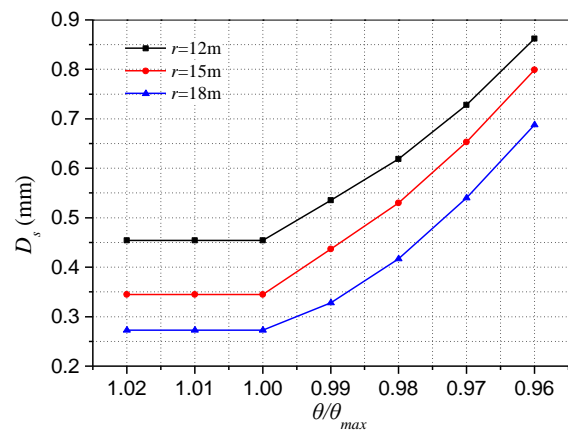


Fig. 7 - Local shear displacements with different frictional angles of fault

The shear displacements of nodes at where  $r = 12\text{m}$ ,  $r = 15\text{m}$  and  $r = 18\text{m}$  in the 7 cases are presented in Figure 7, which donates sensitivity of the rock shear behaviour to the fault shear strength. With frictional angle decreased, the shear displacements of nodes kept constant when  $\theta / \theta_{max} \geq 1.00$ , and increased when  $\theta / \theta_{max} < 1.00$ , which validated the proposed rock slip criterion in an intuitive way.

### ADDRESSING THE IMPORTANT PARAMETERS RELATED TO ROCK-SLIP INSTABILITY PROBLEMS

It is found in Equation 6 that, the lower limit frictional angle of a fault to maintain rock stability related to rock slip along fault plane when tunnelling in hard rock is determined by 3 parameters, including the horizontal stress ratio  $k$ , dip angle of the fault  $\beta$  and the distance between the fault plane and circular tunnel center  $d$ . To obtain a more comprehensive understanding of the effects of these parameters, a parametric analysis was conducted. The tunnel radius  $r_0$  and vertical stress  $\sigma_z$  were set at 5m and 4MPa, respectively.

#### The effects of fault dip angle

It can be seen in Figure 8 that to keep host rock from sliding at excavation wall, the same lower limit frictional angle  $\theta_{lim}$  is required with different dip angle of the fault. And for different dip angle  $\beta$ ,  $\theta_{lim}$  along the fault plane show different tendency: when fault spatially extends with a very small  $\beta$ ,  $\theta_{lim}$  increases all the way from infinite field to the excavation wall (e.g.  $\beta = 10^\circ$ ), while for  $30^\circ < \beta < 80^\circ$ ,  $\theta_{lim}$  increases firstly and then decreases in the same range. And in the far field (about

$\alpha < 0.1$ ), the lower limit frictional angle  $\theta_{lim}$  shows a great disparity with different fault dips and changes little along the fault plane, which can be explained that the stress distribution far away from tunnel is much less disturbed by excavation, and the required shear strength of fault ( $\theta_{lim}$ ) is mainly determined by the initial stress field. The relation between dip angle and lower frictional angle of fault strongly suggests that fault with dip angle in the vicinity of  $60^\circ$  may be identified to be the most unfavourable to the stability problems of tunnels in terms of the rock slip along fault.

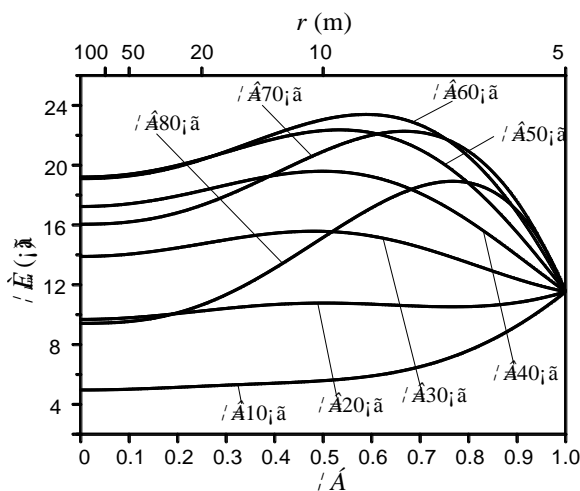


Fig. 8: Lower limit friction angle  $\theta_{lim}$  along fault plane with different  $\beta$  ( $k=0.5, d=1m$ )

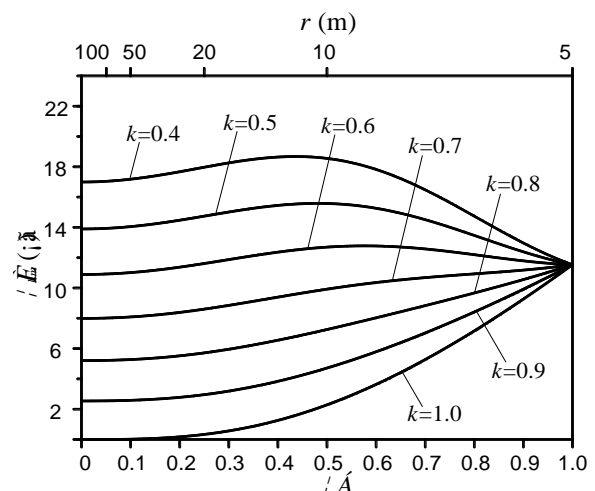


Fig. 9: Lower limit friction angle along fault plane  $\theta_{lim}$  with different  $k$  ( $\beta=30^\circ, d=1m$ )

### The effects of horizontal stress ratio

It has been found that the rock slip was very sensitive to the horizontal stress ratio  $k$  of ground [21], and the input fault shear strength had to be set significant large to reach model equilibrium. By nature, the rock slip along fault is caused by relative insufficient fault shear strength which is also closely related to stress ratio. Therefore, the effects of horizontal stress ratio on the lower limit frictional angle should be investigated.

The lower limit frictional angle of fault in the far field is strongly dependent on horizontal stress ratio as presented in Figure 9, and it increases with the decrease of horizontal stress ratio from 1.0 to 0.4 in detail. From all the cases, it can be summarized that with horizontal stress ratio closer to 1.0, higher stability of host rock related to fault could be expected.

The relation between lower limit angle and horizontal stress ratio in Figure 9 is similar to that of Figure 8, which is: the lower limit frictional angle is strongly dependent on horizontal stress ratio in the far field ( $\alpha$  approaches 0), while that of fault at excavation wall are the same in each figure. According to the relations presented in Figure 8 and Figure 9, it suggests that, the lower limit frictional angle of fault to keep host rock from sliding at excavation wall seems independent of horizontal stress ratio and fault dip angle. However, it should be noted that, rock slip along fault plane is dependent on the shear strength of the whole fault, and the rock near excavation wall is in a loose

state somehow. Given this comprehension, horizontal stress ratio and fault dip angle are also critical for the instability problem of underground excavation related to fault.

### The effects of fault spatial location

Stress redistribution induced by excavation is significant around the tunnel, which means that the stress components on the fault plane near excavation wall are strongly affected. And thus the stress components along the fault plane near the excavation wall should be different with different fault spatial location with respect to the tunnel, which might lead to changes of the required shear strength of fault  $\theta_{lim}$ .

As presented in Figure 10, with different fault spatial locations,  $\theta_{lim}$  approaches the same value of  $13.90^\circ$  when  $\alpha$  approaches 0, and it suggests that in the far field, the stress components of on fault plane is not affected by fault location with respect to tunnel. While when  $\alpha$  approaches 1 (near the excavation wall),  $\theta_{lim}$  changes significantly with different  $d$  (e.g.  $\theta_{lim, d=0.1m} \approx 1.2^\circ$  and  $\theta_{lim, d=2m} \approx 23.5^\circ$ ). And this is remarkable evidence that the instability problems of tunnels in terms of rock slip in the vicinity of excavation wall are dominated by the distance between fault plane and tunnel center.

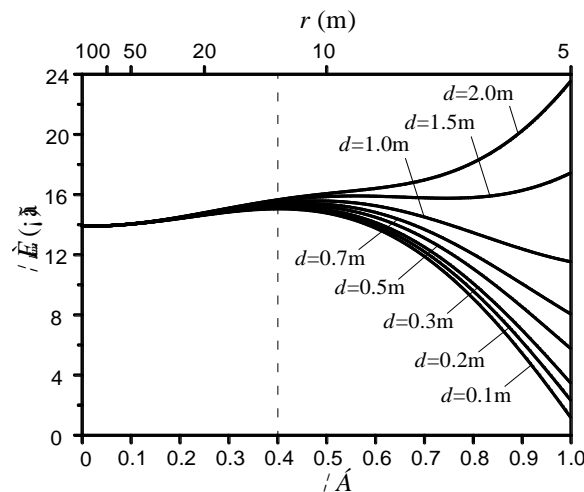


Fig. 10 - Lower limit friction angle along fault plane  $\theta_{lim}$  with different  $d$  ( $\beta=30^\circ, k=0.5$ )

### CHARACTERISTICS OF SHEAR DISPLACEMENTS INDUCED BY TUNNELING

Once rock slip along the fault plane appears, the tunnel support might be subjected to significant nonuniform rock deformation which would result in unfavourable load on support. By taking this into consideration, the tunnelling-induced nonuniform rock deformation related to fault is characterized by using numerical simulations.

The numerical analysis was focused on the parameters of fault dip angle, horizontal stress ratio and the distance between fault plane and circular tunnel center. Another important parameter was the shear strength of fault (for fault in hard rock, the cohesion could be neglected). To stabilize the rock slip far away from excavation wall along fault plane, the frictional angle of fault should be larger than a certain value (called  $\theta_{ini}$ , short for the initial required frictional angle of a fault) which could be calculated by Equation 6 with  $\alpha = 0$ . Given this understanding, the frictional angle of the fault in the numerical analysis should be not less than  $\theta_{ini}$ .

In the numerical cases, prior to tunnel excavation, the model was applied to ground stress at boundaries to reach equilibrium and to produce the in situ stress field. As the proposed criterion was based on elasticity assumption, the models were assumed to be elastic media (other properties of rock and fault are listed in Table 1 and Table 2. In the initial stress equilibrium process, the frictional angle of the fault was the main parameter that affects the equilibrium of the whole system with specified stress boundary conditions and spatial extension and location of a fault. After model equilibrium was reached, the tunnel was excavated in one step and the model was solved for a following equilibrium.

### Shear displacements induced by tunnelling related to fault shear strength

It is obvious that the tunnelling-induced shear displacements are determined by the shear strength of a fault. The fault frictional angle might be larger than  $\theta_{max}$ , or in the range of  $\theta_{ini}$  to  $\theta_{max}$ , or less than  $\theta_{ini}$ , when in-situ combinations of ground horizontal stress ratio and fault spatial extension and location (i.e. fault dip angle and the distance between fault plane and tunnel center) are specified. To analyse the tunnelling-induced shear displacements, the input  $\theta$  should not exceed  $\theta_{max}$ . The frictional angle of the fault  $\theta$  was reduced from  $\theta_{max}$  to  $\theta_{ini}$  with an interval of  $2\% \times (\theta_{max} - \theta_{ini})$ . The variations of shear displacements  $D_s$  at excavation wall (as located in Figure 5) induced by tunnelling are summarized in Figure 11.

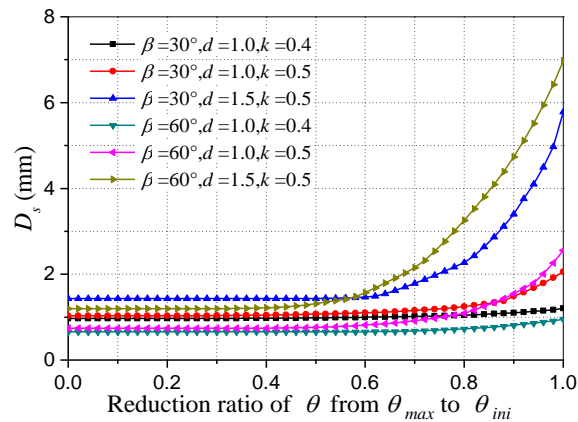


Fig. 11 - Shear displacements at excavation wall varying with gradual reduction of fault shear strength for different combinations of horizontal stress ratio and fault spatial extension and location

It could be seen in Figure 11 that, the shear displacements at excavation wall with different combinations of horizontal stress ratio and fault spatial extension and location show similar tendency. With gradually reduction of the input frictional angle of the fault, tunnelling-induced shear displacements increase only when the reduction ratios exceed about 0.4, and this phenomenon might be attributed to a stress redistribution process that, part of shear stress of slip-failure zones were transferred to nearby zones, and then the distinguishable rock slip was delayed. For cases in Figure 11 with larger distances between fault plane and tunnel center, tunnelling-induced shear displacements are much larger than that of other cases when fault frictional angles are reduced to  $\theta_{ini}$ .

### The effects of fault dip angle

To reveal the effects of fault dip angle or horizontal stress of ground on the tunnelling-induced shear displacement at excavation wall, other important parameters in the numerical models should be given fixed values. As discussed before, the input frictional angle of fault should be in the range of from  $\theta_{ini}$  to  $\theta_{max}$ . And for remarkable shear displacements from the numerical models, the input shear strength of the fault should better to be set at  $\theta_{ini}$  according to Figure 11. The relationship between the initial required frictional angle  $\theta_{ini}$  and horizontal stress ratio and fault dip angle graphically presented in Figure 12, however, shows that for a fixed dip angle of fault, there is no identical  $\theta_{ini}$  could be approached when stress ratio changes. And this is a sign that analysing the effects of stress ratios on the tunnelling-induced shear displacement was hard to be performed. On the other hand, for a fixed stress ratio, there is identical a  $\theta_{ini}$  that could be approached, which indicates that the analysis on the effect of fault dip angle on the tunnelling-induced shear displacement is practicable. 5 combinations of horizontal stress ratios and dip angles of faults are

presented in Figure 13 to demonstrate case pairs in the analysis on the effect of dip angle. And the case conditions of each combination were set with identical stress ratio and input frictional angle of fault.

The fault dip angle is a main parameter that characterizing the spatial extension of a fault, which has a dominant influence on the ground stress distribution. And the rock deformations may show some different characteristics when tunnelling. Figure 14 demonstrates the shear displacements induced by tunnelling with different fault dip angles while other parameters in the models are fixed. It's clearly seen that, fault dips have remarkable influences on the tunnelling-induced shear displacements in each dip pairs. It also could be found that, the shear displacements in each pair of numerical models with larger dip angles are larger than that of models with smaller dip angles. And when the dip angles in each pair are getting closer, the differences of shear displacements get smaller.

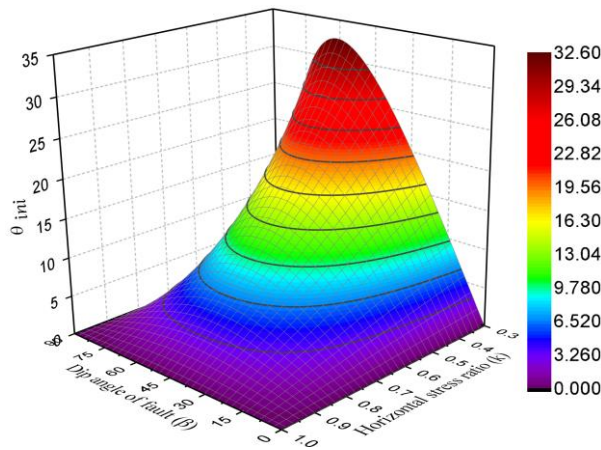


Fig. 12 - Variation of the initial required frictional angle of fault  $\theta_{ini}$  with stress ratio of ground and dip angle of fault

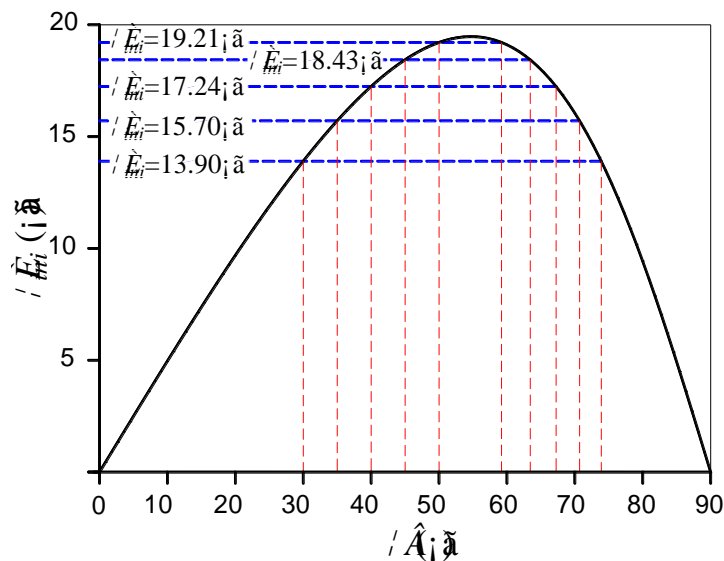


Fig. 13 - Variation of the initial required frictional angle of fault  $\theta_{ini}$  with dip angle of fault ( $k = 0.5$ )

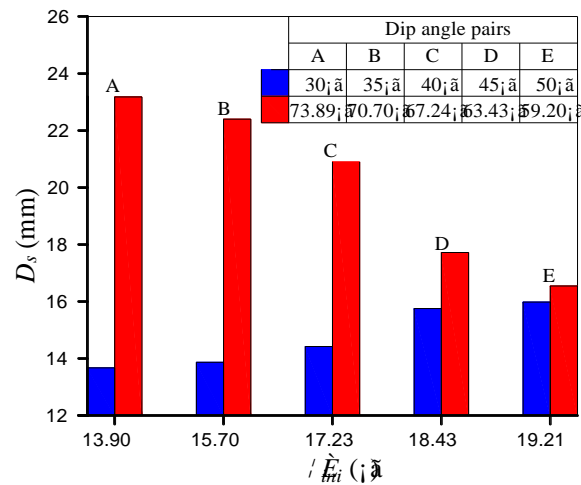


Fig. 14 - Relationship between tunnelling-induced shear displacements and different fault dip angle pairs ( $k = 0.5, d = 2.0\text{m}$ )

It should be noted that, the effects of fault dip on the tunnelling-induced shear displacements  $D_s$  was investigated just for individual dip angle pairs that determined the same  $\theta_{ini}$  as the input frictional angle of a fault. And no relationship of shear displacements varying with continuous variation of fault dip angle was investigated. However, it still could be concluded that, larger fault dip angle ( $\beta > 55^\circ$  for specified stress ratio and spatial extension of a fault, according to Figure 13) is not favourable to the stability of host rock of tunnel related to fault when compared to the corresponding smaller one.

### The effects of fault location

The distance between tunnel center and fault plane  $d$  in detail, is an important parameter that characterizes the fault relative spatial location. As has been discussed before, only the lower frictional angle of a fault near the excavation wall was strongly affected by  $d$  (Figure 10). Then, the effect of  $d$  on the shear displacements could be investigated by giving fixed fault dip angles and horizontal stress ratios.

Results of the four cases with  $d$  increased from 0m to 3m presented in Figure 15 show similar tendencies, which could be described as: further the fault plane is away from tunnel center (no larger than the tunnel radius), larger shear displacement  $D_s$  induced by tunnelling at excavation wall could be expected. And the relationship of shear displacement varying with  $d$  indicates that, when tunnelling in faulted hard rock, fault location with respect to tunnel has a dominant influence on the stability of rock near where fault intersecting with tunnel.

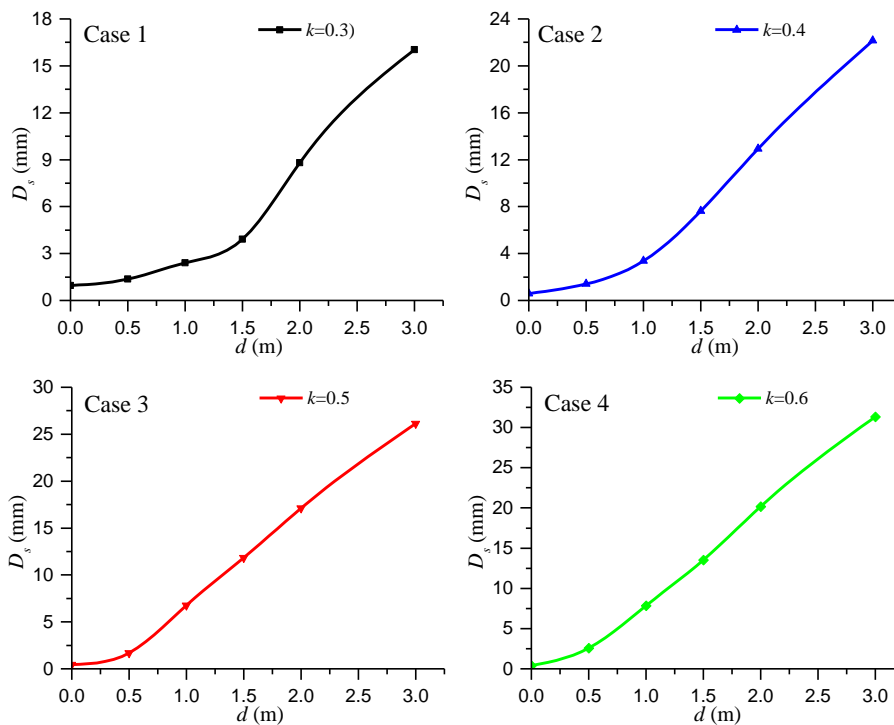


Fig. 15 - The relationship of shear displacements varying with  $d$  ( $\beta=50^\circ$ )

The 4 cases are modelled with different horizontal stress ratio and it seems that, larger stress ratio results in larger shear displacement. However, this apparent phenomenon could be explained by Figure 9 that, with a stress ratio closer to 1, the  $\theta_{ini}$  input into the numerical model is smaller and resulting in larger shear displacements.

## CONCLUSIONS

Based on continuum assumption and Coulomb-slip criterion, analysis of stress on the fault plane was carried out, and then a criterion to evaluate rock slip along the fault for a circular tunnel, which was excavated in rock mass containing a fault was proposed. The proposed criterion was validated through numerical models. By mathematically describing the proposed rock slip criterion, the “lower limit frictional angle of a fault” parameter was put forward, which was the required shear strength of local part of a fault to prevent rock slip. The main advantage of the proposed criterion is that the potential rock slip along a fault around a circular tunnel could be evaluated by simple calculations and comparisons. By theoretical analysis and numerical explorations, deeper insight into the fault-related instability problems of tunnels is provided, which could be summarized as below:

The fault shear strength was proved to be the main parameter that controlled the stability of rock mass around the tunnel, when compared to required shear strength (the lower limit frictional angle of a fault). The required shear strength of a fault is determined by horizontal stress ratio of ground and the spatial extension and location of a fault, and the analysis of these important parameters’ influences on the lower frictional angle of a fault suggested that the rock slip instability near the excavation wall was strongly dependent on the fault spatial location. And this phenomenon was also demonstrated by the effect of fault location on the tunnelling-induced shear displacements near the excavation wall, as larger shear displacement appeared with larger distance between tunnel center and fault plane.

Fault dip in relation to the tunnel was proved to be an important parameter, which the required shear strength of the fault is dependent on. It is demonstrated that, the rock slip stability along the whole fault was influenced by the fault dip. Besides, the tunnelling-induced shear displacement at excavation wall with greater fault dip angle ( $0^\circ < \beta < 90^\circ$ ) was larger than that of the smaller corresponding fault dip with which the other parameters of the numerical models could be set as the same values.

The effect of ground stress ratio also showed great influence on the stability problem of tunnels in faulted rock masses. With the stress ratio closer to hydrostatic stress state, the required shear strength of a fault is much smaller in the far field. Meanwhile, the required shear strength of a fault near the excavation wall is affected by the ground stress ratio much less, as it is mainly determined by fault location.

Generally, the present research is based on elastic mechanics, and thus no plastic behaviour of rock could be considered, which might be the main limitation of this research. And if the plastic behaviour of rock could be taken into consideration, further explorations of the fault-related instability problems of tunnels could be more comprehensive and useful.

## ACKNOWLEDGEMENTS

This paper was sponsored by the National Natural Science Foundation of China (Grant No. 51378436). The authors wanted to express thanks to the foundation.

## REFERENCES

- [1] Bruneau G., Tyler D., Hadjigeorgiou J, Potvin Y., 2003. Influence of faulting on a mine shaft—a case study: part I—Background and instrumentation. *International Journal of Rock Mechanics and Mining Sciences*, vol. 40: 95-111
- [2] Meng L., Li T., Jiang Y., Wang R, Li Y., 2013. Characteristics and mechanisms of large deformation in the Zhegu mountain tunnel on the Sichuan–Tibet highway. *Tunnelling and Underground Space Technology*, vol. 37: 157-164
- [3] Kun M., Onargan T., 2013. Influence of the fault zone in shallow tunneling: A case study of Izmir Metro Tunnel. *Tunnelling and Underground Space Technology*, vol. 33: 34-45
- [4] Suorineni F., Tannant D., Kaiser P., 1999. Determination of fault-related sloughage in open stopes. *International Journal of Rock Mechanics and Mining Sciences*, vol. 36: 891-906
- [5] Brekke T.L., Howard T.R., 1972. Stability problems caused by seams and faults. *International Journal of Rock Mechanics & Mining Sciences & Geomechanics Abstracts*, vol. 12: 95
- [6] Nagelhout A.C.G., Roest J.P.A., 1997. Investigating fault slip in a model of an underground gas storage facility. *International Journal of Rock Mechanics & Mining Sciences*, vol. 34: 212.e211–212.e214
- [7] Li D., Xia B.W, Hao C., Bai S.W., 2009. Research on stability of tunnel in anisotropic layered rockmass with low inclination angle bedding by model test. *Rock & Soil Mechanics*, vol. 30: 1933-1938
- [8] Brekke T.L., Howard T.R., 1974. Functional classification of gouge materials from seams and faults in relation to stability problems in underground openings : 65F, 18T, 84R. US BUR. MINES, TECHNICAL REPORT, 1973. *International Journal of Rock Mechanics & Mining Sciences & Geomechanics Abstracts*, vol. 11: 62-62
- [9] Moretto, O., 1993. A case history in Argentina – rock mechanics for the underground works in the pumping storage development of Rio Grande No. 1 *Comprehensive Rock Engineering*, vol. 5. Pergamon Press, Oxford
- [10] Barton N., Lien R., Lunde J. (1974) Engineering classification of rock masses for the design of tunnel support. *Rock Mechanics*, vol. 6: 189-236
- [11] Brady, B.H.G., Brown, E.T., 1993. *Rock Mechanics for Underground Mining*, second ed. Chapman & Hall, London
- [12] Goodman, R.E., Shi, G.H., 1985. *Block Theory and its Application to Rock Engineering*. Prentice-Hall, Englewood Cliffs, NJ. p. 338
- [13] Sun X.L., Wang H.Z., 2006. 3D FEM analysis of horizontal jet grouting prelining in a tunnel under

- asymmetric loads. *Tunnelling & Underground Space Technology*, vol. 21: 366-367
- [14] Xiao J.Z., Dai F.C., Wei Y.Q., Min H., Xu C., Tu X.B., Wang M.L., 2014. Cracking mechanism of secondary lining for a shallow and asymmetrically-loaded tunnel in loose deposits. *Tunnelling & Underground Space Technology*, vol. 43: 232-240
- [15] Zhou X.J., Gao Y., Li Z.L., 2006. Experimental study on the uneven rock pressure and its distribution applied on a tunnel embedded in geologically bedding strata. *Modern Tunnelling Technology*, vol. 41: 12-21
- [16] Huang F., Zhu H., Xu Q., Cai Y., Zhuang X., 2013. The effect of weak interlayer on the failure pattern of rock mass around tunnel – Scaled model tests and numerical analysis. *Tunnelling and Underground Space Technology, incorporating Trenchless Technology Research*, vol. 35: 207-218
- [17] Zhu Z.Q., Qian S., Mei S.H., Zhang Z.R., 2009. Improved ubiquitous-joint model and its application to underground engineering in layered rock masses. *Rock & Soil Mechanics*, vol. 30: 3115-3121+3132
- [18] Bhasin R., Hoeg K., 1998. Parametric study for a large cavern in jointed rock using a distinct element model (UDEC—BB). *International Journal of Rock Mechanics & Mining Sciences*, vol. 35: 17-29
- [19] Jeon S., Kim J., Seo Y., Hong C., 2004. Effect of a fault and weak plane on the stability of a tunnel in rock—a scaled model test and numerical analysis. *International Journal of Rock Mechanics & Mining Sciences*, vol. 41: 658-663
- [20] Yeung M.R., Leong L.L., 1997. Effects of joint attributes on tunnel stability. *International Journal of Rock Mechanics & Mining Sciences*, vol. 34: 348.e341–348.e318
- [21] Hao Y.H., Azzam R., 2005. The plastic zones and displacements around underground openings in rock masses containing a fault. *Tunnelling & Underground Space Technology*, vol. 20: 49-61
- [22] Wang X., Kulatilake P.H.S.W., Song W.D., 2012. Stability investigations around a mine tunnel through three-dimensional discontinuum and continuum stress analyses. *Tunnelling and Underground Space Technology, incorporating Trenchless Technology Research*, vol. 32: 98-112
- [23] Jia P., Tang C.A., 2008. Numerical study on failure mechanism of tunnel in jointed rock mass. *Tunnelling & Underground Space Technology, Incorporating Trenchless Technology Research*, vol. 23: 500-507
- [24] Zhang Z., Chen F., Li N., Swoboda G., Liu N., 2017. Influence of fault on the surrounding rock stability of a tunnel: Location and thickness. *Tunnelling and Underground Space Technology, incorporating Trenchless Technology Research*, vol. 61:1-11
- [25] Xu D.P., Feng X.T., Cui Y.J., Jiang Q., 2015. Use of the equivalent continuum approach to model the behavior of a rock mass containing an interlayer shear weakness zone in an underground cavern excavation. *Tunnelling and Underground Space Technology*, vol. 47: 35-51
- [26] Kirsch E.G., 1898. Die Theorie der Elastizität und die Bedürfnisse der Festigkeitslehre. *Z VDI. Zeitschrift Des Vereines Deutscher Ingenieure*, vol 42:797-807
- [27] Jiang Y., Tanabashi Y., Li B., Xiao J., 2006. Influence of geometrical distribution of rock joints on deformational behavior of underground opening. *Tunnelling and Underground Space Technology, incorporating Trenchless Technology Research*, vol. 21: 485-491
- [28] Itasca Consulting Group Inc., 2004. UDEC (Universal Distinct Element Code), Version 4.0, User Manual. Itasca Consulting Group Minneapolis, MN, USA
- [29] Jiang Y., Nakagawa M., Esaki T., 2010. Quantitative evaluation of mechanical properties of the natural rock joints for analyzing behavior of structures in discontinuous rock masses. In: *Proceedings of JSCE*, vol. 624: 231-243
- [30] Jiang Y., Xiao J., Tanabashi Y., Mizokami T., 2004. Development of an automated servo-controlled direct shear apparatus applying a constant normal stiffness condition. *International Journal of Rock Mechanics & Mining Sciences*, vol. 41: 275-286
- [31] Kulatilake P.H.S.W., Ucpirti H., Wang S., Radberg G., Stephansson O., 1992. Use of the distinct element method to perform stress analysis in rock with non-persistent joints and to study the effect of joint geometry parameters on the strength and deformability of rock masses. *Rock Mechanics & Rock Engineering*, vol. 25: 253-274